Available online at www.sciencedirect.com
SCIENCE DIRECT®
BioSystems 76 (2004) 65–74
BioSystems
www.elsevier.com/locate/biosystems

# Human-like reflex control for an artificial hand

Michele Folgheraiter*, Giuseppina Gini

*Politecnico di Milano, DEI, Piazza Leonardo da Vinci 32, Italy*

Received 28 February 2003; received in revised form 11 July 2003; accepted 1 August 2003

**Abstract**

In this paper, we illustrate the low level reflex control used to govern an anthropomorphic artificial hand. The paper develops the position and stiffness control strategy based on dynamic artificial neurons able to simulate the neurons acting in the human reflex control. The controller has a hierarchical structure. At the lowest level there are the receptors able to convert the analogical signal into a neural impulsive signal appropriate to govern the reflex control neurons. Immediately upon it, the artificial motoneurons set the actuators inner pressure to control the finger joint position and moment. Other auxiliary neurons in combination with the motoneurons are able to set the finger stiffness and emulate the inverse myotatic reflex control. Stiffness modulation is important both to save energy during task execution, and to manage objects made of different materials. The inverse myotatic reflex is able to protect the hand from possible harmful external actions. The paper also presents the dynamic model of the joints and of the artificial muscles actuating Blackfingers, our artificial hand. This new type of neural control has been simulated on the Blackfingers model; the results indicate that the developed control is very flexible and efficient for all kind of joints present in the humanoid hand.


*Keywords:* Reflex control; Neural control; Artificial hand; Humanoid robotics

## 1. Introduction

The aim of this work is the experimentation of a "human-like" control system for an artificial hand. Very few projects have so far investigated the problem of controlling a humanoid hand so as to mimic the human control system.

At MIT, Matsuoka (1995) has developed different learning strategies for the Cog robot. However, the Cog hand is not human-like, but much simpler, with three fingers and a thumb. It is self-contained having four motors and 36 exteroceptor and proprioceptor sensors controlled by an on-palm microcontroller. Primitive manipulation is learned from sensory inputs using competitive learning, back-propagation algorithm and reinforcement learning strategies. Interesting in the work of Matsuoka is the implementation of a reflex control. The curling reflex allows the fingers to curl when the inner surface palm is touched, and a releasing reflex is triggered when an intolerable amount of stimulus is applied. In the implementation, a simple threshold is used for both.

Also Hannaford et al., at University of Washington have experimented for a long time the control of an anthropomorphic artificial arm using a system capable of emulating the human neuro-muscolo-skeletal motion control. These kind of works are useful, not only to design and control a human-like artificial limb, but also to better understand the biological paradigm, as in Hannaford and Chou (1997).

Another interesting project is under development by Kawamura et al. (2000). Their robotic system, ISAC,

* Corresponding author. Tel.: +39 02399 3482.
*E-mail addresses:* folghera@elet.polimi.it (M. Folgheraiter), gini@elet.polimi.it (G. Gini).

0303-2647/$ – see front matter 
doi:10.1016/j.biosystems.2004.05.007

is targeted to aid elderly or disabled people in their homes. ISAC's 6DOF arms thus require anthropomorphic hands. The current implementation utilizes a Watt 6-Bar Linkage for coupling actuator motion for both the distal and proximal joints of a single finger. This allows one actuator to emulate the joint ranges of the proximal and distal joints of the human phalanx. The hand has five force sensitive resistors (FSRs). Each finger's inside distal pad contains an FSR that varies its resistance based on the force exerted on its surface. Additionally, one FSR resides in the palm. The backside of the palm contains the circuitry for the FSRs. A grasping behavior based on the first grasping patterns of the neonates, as seen before, is implemented. Force-Based Grasping is a high level behavior used to grasp objects based on a priori knowledge. A grasping force and a simple Boolean command are given to this behavior. If the fingers close at the given grasping force without registering any forces, this behavior issues an error message for the upper control level.

Other relevant work is underway in Neural Computation, which attempts to combine knowledge from biology with knowledge from physics and engineering, with the goal of discovering new technologies by studying the principles of natural behavior. Movement coordination requires some form of planning: every degree of freedom needs to be supplied with appropriate motor commands at every moment in time. Due to the numerous degrees of freedom in humanoids, and the almost infinite number of possibilities to use them over time, there exists an infinite number of possible movement plans for any given task, making learning quite intractable. Thus, research in trajectory planning has been focusing on an alternative method by requiring that movements be built from movement primitives defined by speed and amplitude parameters, then fine tunes through learning to improve the movement (Shaal, 1999).

Inspiration from biology motivates another project. A common feature in the brain is to employ topographic maps as basic representation of sensory signals. Such maps can be built with various neural network approaches, and learning motor control with topographic maps can follow Kawamura et al. (1999).

None of the above mentioned methods are so far used for the hand control. In the following Section 2, we illustrate our prototype of an artificial hand. In Section 3, we discuss the functional aspects of the muscle control in natural systems, while in Section 4, we present the control strategy based on emulating the reflexes. Section 5 discusses the model description for the artificial hand, while Section 6 develops the models of neurons. In Section 7, we present and discuss the simulation results of a single joint actuated by two artificial muscles. Section 8 gives conclusions and proposes further research.

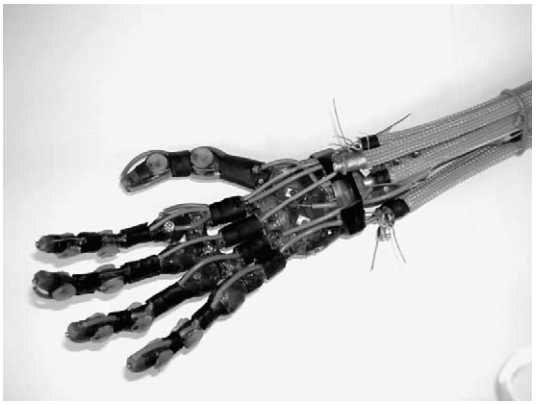

Fig. 1. Blackfingers.

## 2. Our artificial hand

In this paper, we describe the low level control strategy for our prototype of an artificial hand Blackfingers (Fig. 1). As already underlined, the first step of our design was a good understanding of the human hand. After the study of the natural hand, both in bones and muscles organization, we recall here the construction of the artificial hand as in Folgheraiter and Gini (2000).

As in the human hand, the joints of Blackfingers are of two kinds: the spherical ones connect metacarpi to the first phalanxes (and provide 2 d.f.), the cylindrical ones provide rotation. In our hand all the joints have been made from Nyloil (a particular kind of nylon) using a special cutting technique that replicates the natural shapes of of the bone structures. The ligaments were obtained from elastic bands that connect joints, thus allowing them limited movement. The tendons are obtained with iron cables covered with 0.5 mm of Teflon. To connect tendons with the artificial bones plastic bands have been applied. In our prototype each finger is moved by the combined action of six tendons.

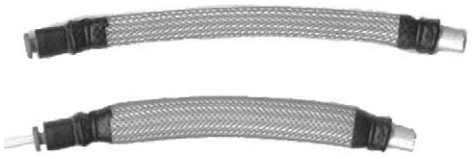

Fig. 2. Actuator release-contraction.

In the first version of the prototype we built a hybrid hydraulic-pneumatic system using six cylinders as actuators for each finger. The precision of the system was good as well as its strength. Nevertheless, for actuating the total of 18° of freedom of the hand (three in each finger and three in the wrist), we needed 36 actuators that we were not able to insert in the forearm. Recently, we have studied and experimented a new version of McKibben actuators, that we have built using light and resistant materials, as in Fig. 2. All the components have been constructed using a polymeric material and aluminum alloy, as we can see in Fig. 2. The actuator's weight is only 20 g, with a good reduction with respect to the 170 g of a traditional pneumatic cylinder.

Also the dimensions are half with respect to the classical actuators, the advantage is that we can maintain the same force and dynamic performance. With this new system we can pack about 40 actuators in a space of only 60 mm × 60 mm × 200 mm, and give the full motion to every hand's joint. Currently, we are working on implementing the position and force sensors directly inside the actuator, to save space and to reduce the wire connections with the control system. This aspect is very important because the electric wires in the joints deteriorate with use due to joint movement and friction. After this short presentation of the hand structure and actuation we are able to introduce the control problem.

## 3. Natural reflex control

The most important human interoceptive reflex is the myotatic reflex, which originates from the neuro-muscular fibers. This reflex is characterized by two phases: a rapid contraction followed by a lower and longer contraction that stabilizes the muscle to a given length. Its principal function is maintaining the joint position fixed and compensating external noise

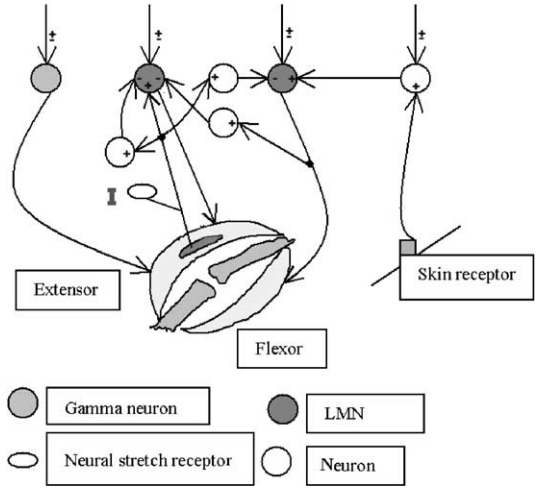


Fig. 3. Schema of a joint with the principal neurons involved in the reflex control.

forces. The other reflex, present in the human beings, is the myotatic inverse reflex; it starts from the Golgi tendon organs and has the main function to inhibit the motoneurons of the given muscle when the strength exceeds dangerous values, as discussed in Atsushi et al. (1991).

In most cases muscles work in opposing pairs: one muscle opens a joint and the other closes it. This configuration is necessary because muscles exert force in one direction only. We can see in Fig. 3, the model of a typical joint with the two antagonist muscles, the spindle inside, the LMN neurons, the gamma neuron, and the interaction between them.

The principal neuron of this system is called the lower motor neuron (LMN). All the neurons illustrated are in the spinal cord, and there are LMN for each muscle fiber. In Fig. 3, we see only one LMN for a muscle. An LMN system must accept commands from many other systems which desire to control the muscle. The degree of contraction of a muscle is proportional to the output pulse frequency of the LMN. The part on the right in Fig. 3 illustrates the simplest type of spinal reflex: a pain receptor in the skin fires a neuron in the LMN system, which in turn fires the LMN driving the flexor muscle. This operation removes the limb from danger. Inhibitory cross connections between the LMNs driving the two muscles insure that they act in concert. This reciprocal synergistic circuitry is generally active in all LMN operations. Higher level

inputs to the LMN system may request such actions as holding a particular position or moving to a specific position. Suppose that the higher nervous center wishes the LMN to maintain a joint at a particular angle. This command reaches a set of constant inputs to the LMN and to the gamma neuron. Now suppose that a load is applied to the finger. This will tend to flex the joint, causing the extensor muscle to be stretched, causing the spindle to be stretched too. Finally, this will increase the output of neuron I, which increases the output of LMN. The resulting increase in the contractive force of the muscle will compensate for the increased load. This kind of local feedback allows the higher system to ignore the fluctuation in contraction required to maintain a certain joint extension.

To develop a neural control for the myotatic reflex we started the construction of a simulator to set the parameters of the reflex control.

## 4. Structure and strategy for our controller

In Fig. 4, we can see the general control structure for a single finger. We can recognize four main blocks: the hand control planner, the low-level control system, the reflex control, and the dynamic model for the finger and for the actuation system.

The finger low-level control receives an high level command from the hand control planner and converts it into a sequence of joint position and force specifications. This control is able also to set the finger stiffness; in this manner it is possible to save energy to maintain a determinate joint position and at the same time execute a specific task. The reflex control block is able to simulate two reflexes that we observe in the human body. In particular, we have simulated the myotatic reflex control and the inverse myotatic reflex control. The last block in Fig. 4 (bottom-right) represents the dynamic model for the finger and for the actuation system.

### 4.1. Reflex control

In this control block we can find all the components necessary for the position and moment control of the joint (Fig. 5). The real position is subtracted from the reference position supplied by the finger dynamic model (Fig. 4); in this manner the position error is obtained. This value is sent to the position receptors for the extensor and flexor actuators, details are in Folgheraiter and Gini (2001). Artificial receptor converts the analog value into a neural impulse signal appropriate for the motoneurons. Another motoneuron's input comes from an auxiliary neuron whose task is to set the joint stiffness. Even if the position error is null, this motoneuron fires with a frequency proportional to the stiffness value that comes from the Low Level Task Control. Another task done by the auxiliary neurons is

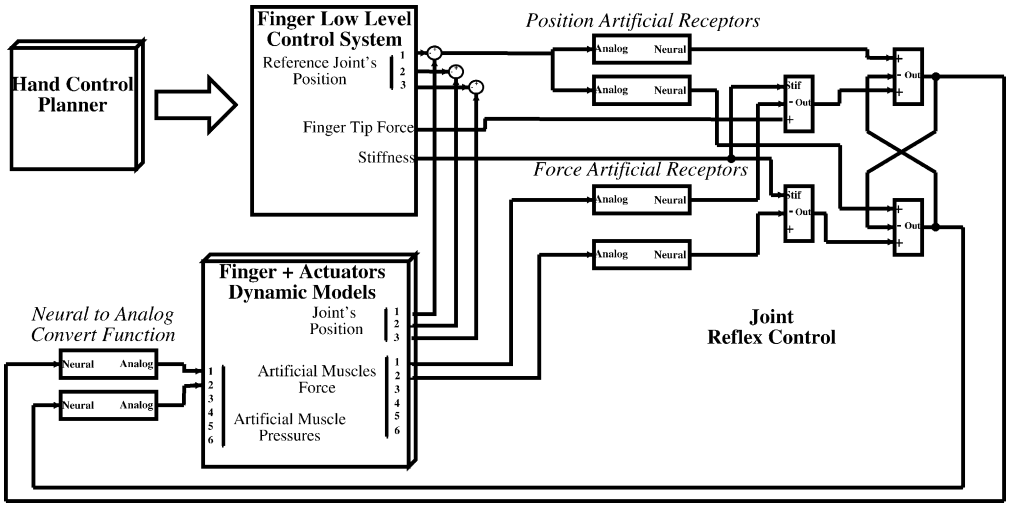


Fig. 4. Low level control general schema.

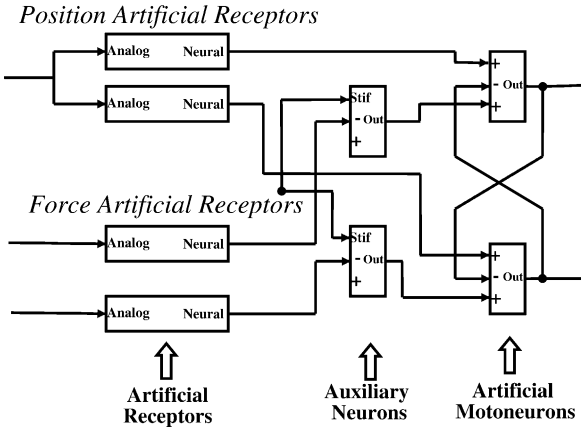


Fig. 5. Artificial miotatic and inverse miotatic reflex control.

to emulate the inverse myotatic reflex, which is based on the two artificial force receptors. As long as the force developed by the actuators is under a threshold, the force-receptor potential is at a low level and consequently it does not fire. However, when the force exceeds the threshold, its potential increases, and so does its firing frequency. The force receptor output, in its turn, feeds an inhibitory input of the auxiliary neuron, so when it starts firing at a high frequency, the auxiliary neuron potential decreases together with its firing frequency. This action inhibits the motoneuron and in turn diminishes the actuator force and the tensions in the flexor and extensor tendons. At this point the joint is free to move under the external action (the joint stiffness is reduced).

This behavior avoids the possibility of damaging the tendons, the actuators and the finger's mechanical structure. It is important to note also the partial motoneuron inhibition due to the output of the antagonist motoneuron (Fig. 5); this circuit ensures that when an actuator is contracted, the other is automatically released.

## 5. Model of the artificial finger

The model has been configured to replicate the finger's joint dynamic, including the actuation system. First, we have empirically obtained the dynamic constants that characterize the dynamics of the real system: elastic constants, friction, inertia, mass, etc. Then we have built the dynamic mathematical model and represented it with the Math works (Matlab) library. Finally after simulations we have set the parameters that characterize the dynamic behavior of the reflex control.

### 5.1. Model of the artificial muscle

This system reproduces the dynamics of the actuation system that is utilized in our artificial hand Blackfinger. Tondu and Lopez (2000) have proposed a good dynamic model for this type of actuators, as in the Eqs. (1) and (2).

$$F_i = \pi r_0^2 P_i[a(1 - K\varepsilon_i)^2 - b] - [f_k + (f_s + f_k)]\,e^{-i/i_s}]\tfrac{1}{n} Sco \cdot P_i \operatorname{sign}(\dot{x}) \quad (1)$$

$$Sco = 2\pi r_0 l_0 \frac{\sin \alpha_0}{(1 - k\epsilon)\sqrt{1 - \cos^2 \alpha_0 (1 - k\varepsilon_i)^2}} \quad (2)$$

where $F_i$ is the force generated from the artificial muscle; $P_i$ the pressure that feeds the actuator, $r_0$ and $l_0$ are the initial radius and length of the muscle, $x$ the muscle position, and $a$, $b$, $\varepsilon$, $f_k$, $f_s$ are other parameters that characterize the muscle structure and the dynamic friction.

### 5.2. Model of the finger joint

The model in Eq. (3) represents the dynamics of the Blackfinger phalanx joint. We have defined the model using the Newton–Euler formulation of dynamics. Like the actuator model, the joint model isn't linear, making it difficult to apply the classic control theories. Instead of working to transform the system into a linear formulation, as in Atsushi et al. (1991), we keep the nonlinear system and develop a neural control as illustrated in the following section.

$$J\ddot{\theta} = -K_e\theta - F_d l + \tfrac{1}{2} mlg \cos\theta + (F_1 - F_2)R \quad (3)$$

where $F_1$, $F_2$ are the artificial muscles forces; $J$ the phalanx inertia moment; $K_e$ the ligament elastic constant; $m$ the phalanx mass; $F_d$ the noise force; $l$ the phalanx length; $R$ the joint radius.

## 6. Model of the artificial neuron

The dynamic neuron model will reproduce the spiking behavior of a natural neuron and is partially based on the Hodgkin and Huxley (1952) and Scholles et al. (1993) models. Eq. (4) gives the general model of our dynamic neuron.

$$\dot{P} = G_1(w_1x_1 - w_2x_2 + w_3x_3 - fP - G_2Th(P))$$
$$Y = G_3Th(P) \tag{4}$$
$$Th(P) = 1, \quad \text{if} \quad P > l_1$$
$$Th(P) = 0, \quad \text{if} \quad P < l_2$$

In the above equation, $P$ represents the action potential of the artificial neuron; its variation is proportional to the inputs frequencies and the inputs weights. The threshold function has a relay behavior: it assumes the value 'one' when the potential exceeds the upper limit $l_1$ and the value 'zero' when the potential is lower than the limit $l_2$; between $l_1$ and $l_2$ the value is equal to the previous state. $X_1$ and $x_1$ are the excitatory inputs, whereas $x_2$ is an inhibitory input; their values are weighted by $w_1$, $w_2$ and $w_3$. The parameter $G_1$ is a loop gain, and its value can modify the dynamic neuron's response.

Like the natural one, the artificial neuron has a short-term memory, and the decay term $-fP$ in Eq. (4) determines the rate of "forgetting". Similar to the input, the output is a sequence of impulses that have the same duration but variable frequency which is a function of the inputs and of the weights values.

In Fig. 6, we can see the simulation of an artificial neuron implementing a motoneuron. Starting from the top the first three signals are neuron inputs, and the last one is the output.

### 6.1. Dynamic weights

The reflex neural network must be able to adapt to the dynamic characteristics of the system that needs to be controlled. In order to perform this behavior, neuron weights have to be changed during the system operation. Their values will change until they reach the optimal solution for the control. This means that the error must decrease as fast as possible, and no overshoot can be present in the system response.

In supervised learning, the adjustment of neuron weights happens in concomitance with function minimization; that is significant for the control problem in question. Instead, in unsupervised learning, the neural network improves its performance

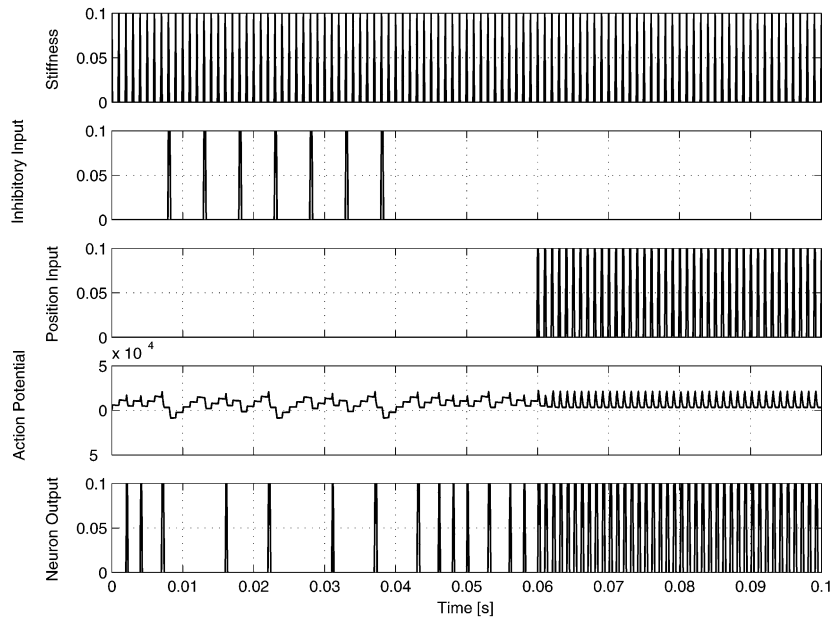


Fig. 6. Neuron response.

using a task-independent measure of the control quality.

However, this process usually is difficult to perform in real time, especially if the network has to learn and control the system at the same time. What we have tried to do in our neuron model is to use dynamic input weighting. In this specific case, the weight is also a dynamic system, and the model in the Laplace domain is presented by the Eq. (5).

$$w_i = \mathrm{Lim}\left(\frac{1}{s}[K_1 x_i - K_2 w_i]\right)$$

$$\mathrm{Lim}(V) = V, \quad \text{if} \quad V_{\min} \leq V \leq V_{\max} \tag{5}$$

$$\mathrm{Lim}(V) = 0, \quad \text{if} \quad V < V_{\min}$$

$$\mathrm{Lim}(V) = 1, \quad \text{if} \quad V > V_{\max}$$

where $K_1$ and $K_2$ are opportunely chosen to set the "correct" learning rate. In fact, if $K_1$ is too big, the weight saturates rapidly at the maximum value permitted.

It is possible to set these two values empirically; let's suppose that the weight input $x_i$ (spiking signal) has the maximum frequency, we want that, in these initial conditions, the weight increases and reaches the maximum value admissible (one) in about 1 s. This specification is sufficient to set the $K_1$ value. In the same mode we can set the $K_2$ value, but this time we have to consider a null $x_i$ input signal and choose the period of time that the weight needs to pass from the high value to the low admissible value (zero). In Eq. (5) the function Lim is an output limitation, and it regulates the internal status of the weight.

The weighting differs from the Hebbian learning rule (Hebb, 1949), because it does not take into account the correlation between the presynaptic and postsynaptic neuron activity. In fact, we can think at this learning rule as a local observer: the weight is reinforced if the input of the neuron is stimulated, and weakened otherwise. In a certain manner each neuron is an independent controller and it realizes the control strategy taking in account only his own inputs. This simplify the network configuration and avoids the weight saturation.

### 6.2. Artificial receptor

This function is able to convert an analog signal into impulse signals that are appropriate to feeds the neurons. Its formula is expressed by the differential Eq. (6).

$$Y = Th(R)$$

$$\dot{R} = x\left[1 - \left(Th(R)\frac{1}{x} + Th(R)\right)\right] \tag{6}$$

$$R(0) = 0$$

$R$ is an internal state, $x$ the input signal, and the threshold function is the same as in Eq. (4). When the state $R$ is lower than a preset value $l_2$, $R$ gets the value of the integration of the input signal $x$, and $Y$ remains at zero value. If $S$ overcomes the $l_1$ limit, the threshold function assumes the value of one, and so does the output $Y$. The impulse duration is a constant independent from the input signal; the impulse frequency instead is proportional to the input intensity. In this manner, we are able to have an impulse signal that has a frequency directly proportional to the analog input value.

### 6.3. Neural to analog function

With this function it is possible to convert an impulse neural signal into a continuous analog signal. The formula that describes this function is expressed by Eq. (7) in the Laplace transform domain.

$$Y(s) = G\frac{1}{0.08s + 1} \tag{7}$$

In this function, the choice of the pole frequency is very critical; if it is too high, there is no integration of the input signal, while if it is too low, the output will not be continuous but will have an impulse behavior.

## 7. Model simulation

To test our control system we have used the Simulink software. Simulation is performed on AMD Athlon 1GHz computer, equipped with 256 Mbytes of RAM. To integrate the differential equations we chose the Euler method with an integration step of 0.1 ms. We have simulated two types of control behavior: the

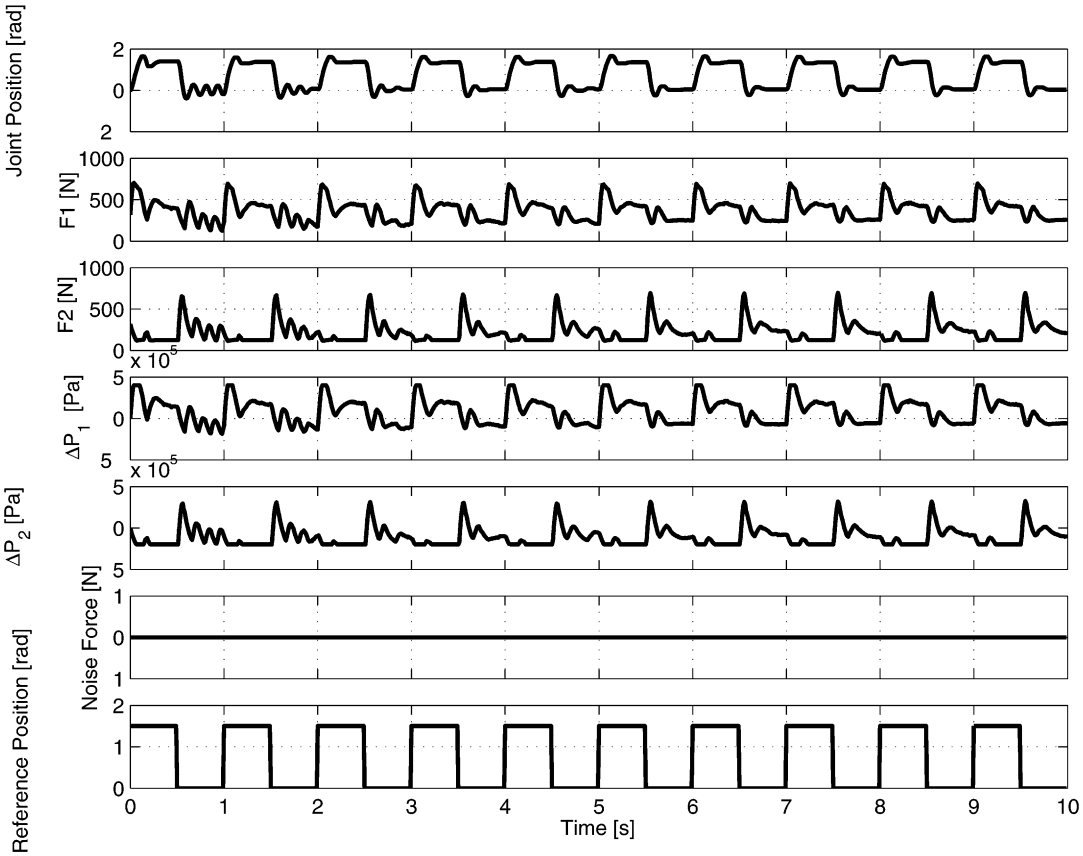


Fig. 7. Myotatic reflex test.

tracking of a reference position for a finger joint and the response to a harmful force.

We can see the results of our first experiment in Fig. 7. In the figure, at the bottom, we can see the reference position (radians) that changes like a square wave whose amplitude is 1 rad and period is 0.5 s. At the top there is the real joint finger position that follows the reference position with appreciable precision. This result is good considering the global system characteristics, in particular recalling that the finger joint model and the actuators model are non linear. The other quantities represented in the graphic output are the forces and the inner pressures of the actuators.

The actuator inner pressure is set by the output of the neural to analog function.

The other experiment, illustrated in Fig. 8, was to test the artificial inverse myotatic reflex. To do that, we have fixed the position of the medial and distal finger joints, then we have flexed the first phalanx of 0.5 rad.

In this condition we have applied at the fingertip a noise force of 80 N, that generated a moment dangerous for the hand, especially for the tendons that are designed to support only fixed maximum loads. For the first 1.5 s of the test, the joint settled at a position of 1 rad (57.2°), then the noise force acted at the fingertip. As a consequence, the force of the actuator connected to the flexor tendon increased until the max value of 800 N. In this condition the artificial force receptor connected to the actuators starts firing at high frequency. This action inhibits the auxiliary neuron and the motoneuron that controls the force in this actuator. After the effect of the artificial inverse myotatic reflex, the force is lowered to 600 N, which is acceptable for the flexor tendon.

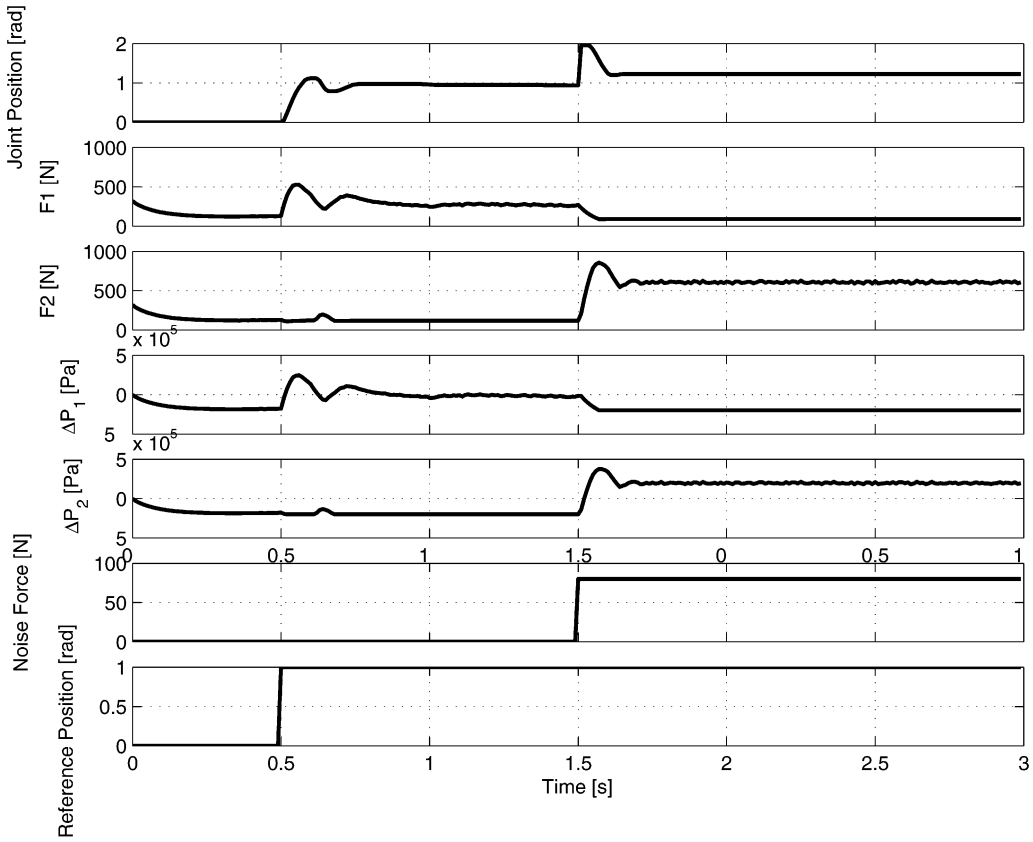


Fig. 8. Inverse myotatic reflex test.

## 8. Conclusion

In conclusion, in this paper, we presented the control system architecture for an artificial hand and the simulation results of its low level controller. In our model we tried to reproduce the structure and the dynamic behavior of the human reflex. We show that the artificial myotatic and inverse myotatic reflexes are reproducible artificially and that their models present a human-like behavior. We demonstrated that in comparison with a classical control system, the reflex control is more easily configurable. This is very important especially if the system that we want to control is non-linear. It is also important to note that the neural network that control the joint stiffness and position of Blackfingers are suitable also for other humanoid robot joints. In comparison with Yong et al. (1996) work, we showed that the myotatic reflex control is applicable to McKibben actuation system, and in the specific case to our prototype of artificial hand. Moreover, in our research, we have developed a specific type of dynamic artificial neuron that has a more human-like response. The next step of our work is to test our control system on the real prototype and compare the experimentation results with the simulation.

## References

Atsushi, Kazuhiko, K., Sugato, B., Mourad, E., August 1991. Reflex control of a robotic aid system to assist the phisically disabled. Symp. Intell. Control.

Folgheraiter, M., Gini, G., September 2000. Blackfingers an artificial hand that copies human hand in structure, size, and function. In: Proceedings of IEEE Humanoids 2000, MIT, Cambridge.

Folgheraiter, M., Gini, G., July 2001. Simulation of reflex control in an anthropomorphic artificial hand. In: Proceedings of

VIII ISCSB 2001 (Int Symposiumon Computer Simulation in Biomechanics), Milan, Italy.

Hannaford, B., Chou, C.-P., 1997. Study of human forearm posture maintenance with a physiologically based robotic arm and spinal level neural controller. Biol. Cybernetics 76, 285–298.

Hebb, D., 1949. The Organization of Behavior: A Neuro-psychological Theory. Wiley, New York.

Hodgkin, A.L., Huxley, A.F., 1952. A quantitative description of membrane current and its application to conduction and excitation in a nerve. J. Physiol. 117, 500–544.

Kawamura, K., II, R.P., Wilkes, D., Alford, W., Rogers, T., July/August 2000. Isac: Foundations in human-humanoid interaction. IEEE Intelligent Systems.

Kawamura, M., Okada, M., Hirai, Y., 1999. Dynamics of selective recall in an associative memory model with one-to-many associations. IEEE Trans. Neural Netw. 10, 704–713.

Matsuoka, Y., 1995. Embodiment and manipulation learning process for a humanoid hand. Master Thesis, MIT.

Scholles, M., Hosticka, B., Kesper, M., Richer, P., Schwarz, M., 1993. Biologically-inspired artificial neurons modeling and applications. Neural Netw.

Shaal, S., 1999. Is imitation learning the route to humanoid robots. Trends Cognitive Sci. 233–242.

Tondu, B., Lopez, P., April 2000. Mckibben artificial muscle robot actuators. IEEE Control Systems Magazine.

Yong, L., Ning, L., Gang, L., 1996. Reciprocal reflex control of equilibrium joint position by antagonistic muscles. 18th Annual Conference of the IEEE Engineering in Medicine and Biology Society, Amsterdam.